Journal of Colloid and Interface Science 327 (2008) 308–315

Contents lists available at ScienceDirect

Journal of Colloid and Interface Science

www.elsevier.com/locate/jcis

Adsorption of direct dyes from aqueous solutions by carbon nanotubes: Determination of equilibrium, kinetics and thermodynamics parameters

Chao-Yin Kuo [a], Chung-Hsin Wu [b,*], Jane-Yii Wu [c]

[a] Department of Environmental and Safety Engineering, National Yunlin University of Science and Technology, Taiwan, ROC
[b] Department of Environmental Engineering, Da-Yeh University, 112, Shan-Jiau Road, Da-Tsuen, Chang-Hua, Taiwan, ROC
[c] Department of Bioindustry Technology, Da-Yeh University, 112, Shan-Jiau Road, Da-Tsuen, Chang-Hua, Taiwan, ROC

ARTICLE INFO

Article history:
Received 25 June 2008
Accepted 20 August 2008
Available online 27 August 2008

Keywords:
Adsorption
Carbon nanotubes
Direct dyes
Isotherm
Kinetics
Thermodynamics

ABSTRACT

This study examined the feasibility of removing direct dyes C.I. Direct Yellow 86 (DY86) and C.I. Direct Red 224 (DR224) from aqueous solutions using carbon nanotubes (CNTs). The effects of dye concentration, CNT dosage, ionic strength and temperature on adsorption of direct dyes by CNTs were also evaluated. Pseudo second-order, intraparticle diffusion and Bangham models were adopted to evaluate experimental data and thereby elucidate the kinetic adsorption process. Additionally, this study used the Langmuir, Freundlich, Dubinin and Radushkevich (D–R) and Temkin isotherms to describe equilibrium adsorption. The adsorption percentage of direct dyes increased as CNTs dosage, NaCl addition and temperature increased. Conversely, the adsorption percentage of direct dyes decreased as dye concentration increased. The pseudo second-order model best represented adsorption kinetics. Based on the regressions of intraparticle diffusion and Bangham models, experimental data suggest that the adsorption of direct dyes onto CNTs involved intraparticle diffusion, but that was not the only rate-controlling step. The equilibrium adsorption of DR86 is best fitted in the Freundlich isotherm and that of DR224 was best fitted in the D–R isotherm. The capacity of CNTs to adsorb DY86 and DR224 was 56.2 and 61.3 mg/g, respectively. For DY86, enthalpy (ΔH^0) and entropy (ΔS^0) were 13.69 kJ/mol and 139.51 J/mol K, respectively, and those for DR224 were 24.29 kJ/mol and 172.06 J/mol K, respectively. The values of ΔH^0, ΔG^0 and E all indicate that the adsorption of direct dyes onto CNTs was a physisorption process.

1. Introduction

Many industries, including textile companies, dye manufacturers, food processing companies, paper and pulp mills, and electroplating factories, release wastewater containing dyes and thereby contaminate water resources. The use of direct dyes has continuously increased in the textile industry and finishing processes since the development of synthetic fibers. Discharging dyes into the hydrosphere typically results in environmental damage as dyes give water undesirable color and reduce sunlight penetration. Additionally, some dyes are toxic to the environment. To minimize the risk of pollution generated by such effluent, this effluent must be treated before discharged into the environment. Many treatment methods have been developed to remove dyes from wastewater. These treatment methods can be divided into physical, chemical and biological schemes. Although chemical and biological approaches are effective in removing dyes, they require special equipment and are usually energy intensive; additionally, these processes often generate large amounts of byproducts. Among all existing techniques, adsorption is considered the most efficient; additionally, adsorption is easily operated and insensitive to toxic substances. Numerous adsorbents, such as algal [1], coir pith [2], wheat shells [3], bentonite [4], compost [5], biogas residual slurry [6], almond shells [7], orange peel [8], soy meal hulls [9] and Fe(III)/Cr(III) hydroxide [10], have been examined for their ability to remove direct dyes from wastewater.

Carbon nanotubes (CNTs) are relatively new adsorbents that can adsorb trace pollutants from wastewater. Recently, CNTs have been characterized as efficient adsorbents with a capacity that surpasses that of activated carbon [11,12]. Considerable attention has focused on adsorption by CNTs of contaminants such as Zn^{2+} [12], Cd^{2+} [13], Pb^{2+} [14,15], Cu^{2+} [15,16], fluoride [17], arsenate [18], trihalomethanes [19], 1,2-dichlorobenzene [20], xylene [21] and dioxin [11]. With the exception of dioxin [11], xylene [21], trihalomethanes [19], 1,2-dichlorobenzene [20] and dyes [22], few studies have examined the adsorption of organic pollutants by CNTs. Hence, two direct dyes, C.I. Direct Yellow 86 (DY86) and C.I. Direct Red 224 (DR224), were selected as adsorbates to determine the adsorption ability of CNTs in this study.

* Corresponding author. Fax: +886 4 8511336.
E-mail address: chunghsinwu@yahoo.com.tw (C.-H. Wu).

0021-9797/$ – see front matter
doi:10.1016/j.jcis.2008.08.038

Table 1
Structure and characteristics of DY86 and DR224

Name	CAS number	C.I. number	Formula	Molecular weight	λ_{max}	Chemical structure
DY86	50925-42-3	29325	$C_{39}H_{30}N_{10}Na_4O_{13}S_4$	1066 g/mol	379 nm	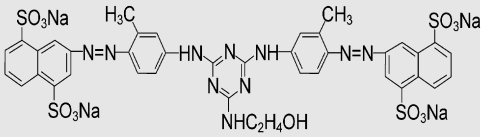
DR224	12222-48-9	Unpublished	Unpublished	Unpublished	518 nm	Unpublished

Understanding adsorption equilibrium, kinetics and thermodynamics is critical to the design and operation of adsorption processes. Early works have presented only equilibrium and kinetic adsorption data and a few studies have measured the thermodynamic parameters of adsorption by CNTs. Li et al. [14] and Peng et al. [20] investigated the thermodynamics of adsorption of Pb^{2+} and 1,2-dichlorobenzene onto CNTs, respectively. Wu [22] and Wu [16] elucidated the thermodynamics of adsorption of C.I. Reactive Red 2 and Cu^{2+}, respectively. Lu et al. [23] analyzed the thermodynamics of adsorption of trihalomethanes by CNTs. Few studies have investigated adsorption of dyes by CNTs and simultaneously determined equilibrium and thermodynamic parameters; however, no study has determined the parameters that govern adsorption of direct dyes. This study elucidates the equilibrium, kinetics and thermodynamics of adsorption of DY86 and DR224 by CNTs. The Langmuir, Freundlich, Dubinin and Radushkevich (D–R), and Temkin isotherms were utilized to fit equilibrium data of adsorption. Adsorption rates were determined quantitatively. Those obtained using the pseudo second-order, intraparticle diffusion and Bangham models were compared. The objectives of this study are to (i) determine the effects of dye concentration, CNT dosage, ionic strength and temperature on adsorption of DY86 and DR224 by CNTs, (ii) measure the coefficients of Langmuir, Freundlich, D–R and Temkin isotherms, (iii) assess the adsorption rate using various kinetic models and (iv) derive changes in thermodynamic parameters-free energy (ΔG^0), enthalpy (ΔH^0) and entropy (ΔS^0) during adsorption.

2. Materials and methods

2.1. Materials

The CNTs used in this study were multi-wall nanotubes (CBT, MWNTs-2040). These CNTs were manufactured by pyrolysis of methane gas on Ni particles via chemical vapor deposition. The C, O and Ni content in CNTs was 90.6, 8.1 and 1.3%, respectively [22]. Surface area, average pore diameter and pore volume was 82.2 m^2/g, 2.5 nm and 1.07 cm^3/g, respectively [16]. The CNTs were 5–15 μm long and the mass proportion of amorphous carbon in CNTs was less than 2%. The parent compounds, DY86 and DR224, were purchased from the Everlight Industrial Chemical Company. Table 1 presents the structure and characteristics of DY86 and DR224. Notably, NaCl was used to control ionic strength. All materials were used as received without further purification. All solutions were prepared using deionized water (Milli-Q) and reagent-grade chemicals.

2.2. Experimental methods

Size and morphology of CNTs were determined by transmission electron microscopy (TEM) using a Philips/FEI Tecnai 20 G2 S-Twin. The pH of the point of zero charge (pH_{pzc}) of CNTs and adsorbed CNTs was measured at pH 3–10 using a Zeta-Meter 3.0 (Zeta-Meter Inc., USA). Ten measurements were made of each sample at each pH and the mean was determined as the zeta potential.

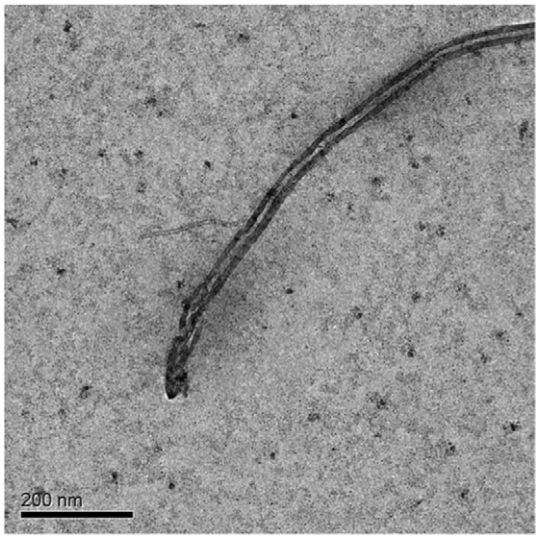

Fig. 1. TEM image of CNTs.

All experiments were conducted in a closed 250 mL glass pyramid bottle. The bottle, which contained 0.1 g of CNTs and 150 mL of dye solution, was placed in a water bath and shaken at 100 rpm. In the experiments to determine the effects of dye concentration (CNTs = 0.67 g/L and $T = 25\,^{\circ}C$), the dye concentration was 10 and 20 mg/L. In experiments on the effect of CNTs dosage (dye = 10 mg/L and $T = 25\,^{\circ}C$), the CNT dose was 0.33 and 0.67 g/L. In experiments to identify the effect of temperature (CNTs = 0.67 g/L and dye = 10 mg/L), temperature was maintained at 15 and 55 °C. At the end of the equilibrium period, suspensions were centrifuged at 4000 rpm for 10 min, and the supernatant was then filtered through 0.2 μm filter paper (Gelman Sciences) for subsequent analysis of dye concentration. Adsorption of DY86 and DR224 was detected using a spectrophotometer (Hitachi-U2001) at 379 and 518 nm, respectively.

3. Results and discussion

3.1. Characteristics of the surface of CNTs

Fig. 1 presents TEM image of CNTs. The outer diameters and inner cavities of CNTs were 20–80 and 5–10 nm, respectively. The TEM analysis verified the hollow structure of CNTs. The pH_{pzc} of CNTs was 4.98 (Fig. 2), which is similar to that measured by Lu and Chiu [12] for multi-wall nanotubes. This analytical result demonstrates that the surface of CNTs was positively charged when solution pH was <4.98. Direct dyes can be classified as anionic dyes. In an aqueous solution, anionic dyes carry negative charges due to the presence of sulfonate (SO_3^-) groups. Therefore, the zeta potentials of DY86 and DR224 adsorbed CNTs were negative at a pH of 3–10, indicating that the CNTs were negatively charged (Fig. 2). Numerous investigations have demonstrated that the zeta potentials of acid-modified CNTs [13,21] and oxidant-modified CNTs [12,13,

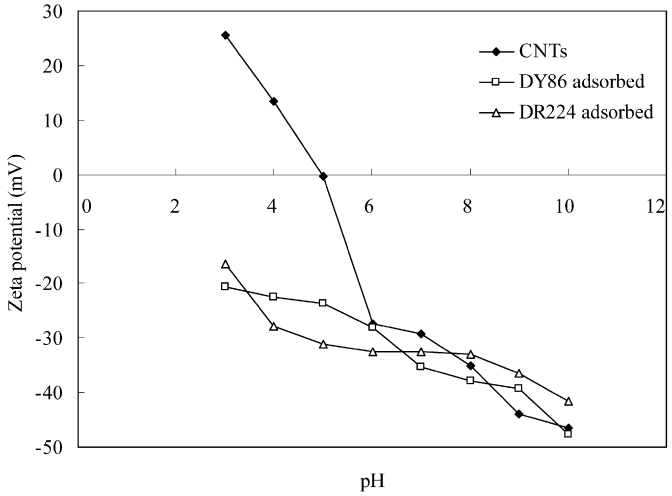

Fig. 2. Zeta potential of raw-CNTs and adsorbed-CNTs.

16] are more negative than those of as-grown CNTs. The surface-modified CNTs may inhibit adsorption of direct dyes onto CNTs due to repulsion of negative charges. Hence, CNTs were used as received without surface modification.

3.2. Kinetics analyses

3.2.1. Effects of dye concentration

Adsorption kinetics, indicating the adsorption rate, is an important characteristic of adsorbents. The adsorption process at different concentrations was rapid in the initial 50 min, and then gradually decreased as adsorption proceeded until equilibrium was reached (Fig. 3). This progression is expected based on the large number of vacant surface sites available for adsorption during the initial stage, and, after certain amount of time, the remaining vacant surface sites are difficult to occupy due to repulsive forces between dye molecules on CNTs and bulk phases [24]. After 240 min of reaction, the adsorption percentage of 10 and 20 mg/L DY86 onto CNTs was 74 and 51%, respectively, and that of DR224 was 79 and 71%, respectively. However, the amount of dye adsorbed per unit of CNT mass increased as initial dye concentration increased due to the increase in the driving force of the concentration gradient for mass transfer with the increase in initial dye concentration. Mall et al. [24] also showed the similar results.

The pseudo second-order, intraparticle diffusion and Bangham models were adopted to test experimental data and thereby elucidate the kinetic adsorption process. The pseudo second-order model is

$$\frac{t}{q} = \frac{1}{k_2 q_e^2} + \frac{t}{q_e}, \tag{1}$$

where q_e and q are the amounts of dye adsorbed onto CNTs at equilibrium and at various times t (mg/g), and k_2 is the rate constant of the pseudo second-order model for adsorption (g/mg min) [22,24]. The slope and intercept of the linear plot of t/q as a function of t yielded the values of q_e and k_2. Additionally, the initial adsorption rate h (mg/g min) can be determined using the equation $h = k_2 q_e^2$. The adsorption process on porous adsorbents generally has four stages—bulk diffusion, film diffusion, intraparticle diffusion and finally adsorption of the solute onto the surface. Typically, bulk diffusion and adsorption are assumed rapid and, therefore, not rate determining. Since the pseudo second-order model cannot identify the diffusion mechanism, kinetic results were analyzed using the intraparticle diffusion model to elucidate the diffusion mechanism. For the intraparticle diffusion model, film diffusion was negligible and intraparticle diffusion was the only rate-controlling step. The intraparticle diffusion model is expressed as

$$q = k_i t^{1/2} + C, \tag{2}$$

where C is the intercept and k_i is the intraparticle diffusion rate constant (mg/g min$^{0.5}$), which can be determined from the slope of the linear plot of q versus $t^{1/2}$ [22,24]. Kinetic data were further utilized to identify the slowness of the adsorption step in the present adsorption system based on Bangham's model [24,25]:

$$\log\left(\frac{C_0}{C_0 - qm}\right) = \log\left(\frac{k_0 m}{2.303V}\right) + \alpha \log(t), \tag{3}$$

where q and t are defined as in the pseudo second-order model, C_0 is the initial dye concentration in the solution (mg/L), V is solution volume (mL), m is the mass of CNTs per liter of solution (g/L), and k_0 and α are constants. Table 2 presents the kinetic parameters for the removal of direct dyes by CNTs. The R^2 value of the pseudo second-order model exceeded 0.96; moreover, the q value

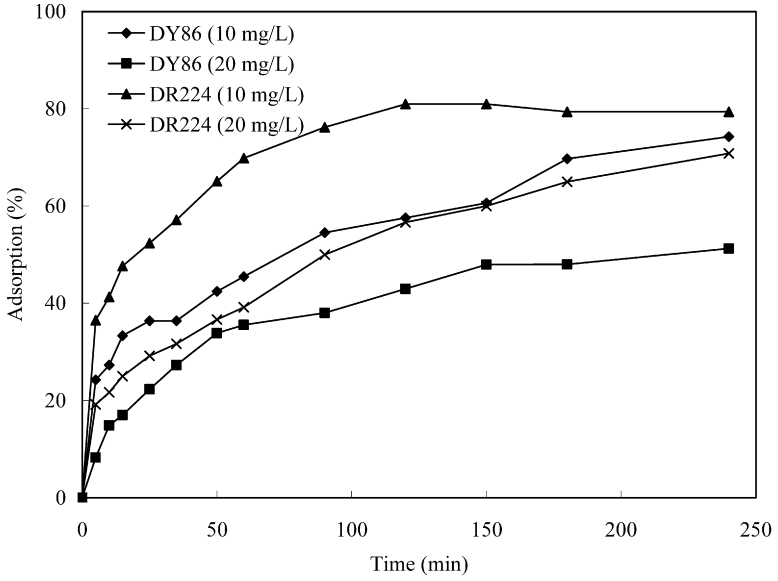

Fig. 3. Effects of dye concentration on the adsorption of direct dyes (CNTs = 0.67 g/L and $T = 25\,^{\circ}C$).

($q_{e,\mathrm{cal}}$) derived from the pseudo second-order model was consistent with experimental q values ($q_{e,\mathrm{exp}}$). Hence, this study suggests that the pseudo second-order model best represents adsorption kinetics. A similar phenomenon has been observed in the adsorption of Acid Blue 93 by natural sepiolite [26], and Acid Red 57 by surfactant-modified sepiolite [27]. If the regression of q versus $t^{1/2}$ is linear and passes through the origin, intraparticle diffusion is then the sole rate-limiting step [24,27]. Although the regression was linear, the plot did not pass through the origin (Table 2), suggesting that adsorption involved intraparticle diffusion; however, that was not the only rate-controlling step. Other kinetic mechanisms may control the adsorption rate, which is a similar finding to that obtained from other studies of adsorption [22,26]. The double logarithmic plot according to the Bangham equation yielded a perfect linear ($R^2 > 0.96$) for the removal of direct dyes by CNTs, indicating that the diffusion of dye into CNT pores is not the only rate-controlling step [28]. The rate constants of the pseudo second-order model (k_2) decreased as the initial concentration of dye in adsorption systems increased. Conversely, the intraparticle diffusion rate constants (k_i) increased as the initial concentration of dye increased. The diverse effects of the initial concentration on k_2 and k_i have also been observed for other adsorption systems [1,29].

Table 2
Kinetic parameters for the removal of direct dyes by CNTs (CNTs dose = 0.67 g/L and $T = 25\,^{\circ}\mathrm{C}$)

Pseudo second-order model	$q_{e,\mathrm{exp}}$ (mg/g)	k_2 (g/mg min)	h (mg/g min)	$q_{e,\mathrm{cal}}$ (mg/g)	R^2
DY86 (10 mg/L)	11.1	2.77×10^{-3}	0.383	11.8	0.972
DY86 (20 mg/L)	15.4	1.58×10^{-3}	0.477	17.4	0.995
DR224 (10 mg/L)	11.9	6.82×10^{-3}	1.099	12.7	0.997
DR224 (20 mg/L)	21.3	1.31×10^{-3}	0.628	21.9	0.962
Intraparticle diffusion model		k_i (mg/g min$^{0.5}$)	C (mg/g)		R^2
DY86 (10 mg/L)		0.57	2.44		0.990
DY86 (20 mg/L)		1.08	1.47		0.971
DR224 (10 mg/L)		0.79	3.91		0.987
DR224 (20 mg/L)		1.24	2.62		0.993
Bangham's model		α	k_0 (L/(mg/L))		R^2
DY86 (10 mg/L)		0.440	2.45×10^{-2}		0.961
DY86 (20 mg/L)		0.523	1.08×10^{-2}		0.986
DR224 (10 mg/L)		0.459	4.03×10^{-2}		0.987
DR224 (20 mg/L)		0.524	1.47×10^{-2}		0.980

3.2.2. Effects of CNTs dosage, ionic strength and temperature

Fig. 4 plots the effects of CNTs dosage on direct dye adsorption. For DY86, the adsorption percentage increased from 42 to 74% when the CNT dosage increased from 0.33 to 0.67 g/L, and for DR224, the adsorption percentage increased from 29 to 79%. The increase in percentage of dye removed with an adsorbent dosage can be attributed to an increase in the adsorbent surface, which increased the availability of adsorption sites. By increasing CNTs dosage from 0.33 to 0.67 g/L, the adsorption of DY86 per unit weight of CNTs decreased from 12.7 to 11.1 mg/g; conversely, the adsorption of DR224 per unit weight of CNTs increased from 8.8 to 11.8 mg/g. The decrease in unit adsorption as adsorbent dosage increased is due to adsorption sites remaining unsaturated during the adsorption process [30]. Another reason for this result may be the overlapping of adsorption sites due to overcrowding of adsorbent particles.

Since large amounts of salts are generally utilized in the dyeing process, the effects of ionic strength on adsorption must be evaluated. Fig. 5 shows the effects of ionic strength on direct dyes adsorption. Experimental results indicate that increasing solution ionic strength increased the adsorption of direct dyes by CNTs. The significant increase in dye removal after adding NaCl can be attributed to an increase in dye dimerization in solutions [31]. Al-Degs et al. [31] indicated that the high adsorption capacity of dyes under salt addition can be attributed to the aggregation of dye molecules induced by the action of salt ions, i.e., salt ions force dye molecules to aggregate, increasing the extent of adsorption of dyes onto CNTs. Moreover, the initial adsorption rate increased significantly at a high ionic strength, implying that direct dyes attachment is controlled by electrostatic interactions.

3.3. Adsorption isotherms

The adsorption isotherm is the most important information, which indicates how adsorbate molecules are distributed between the liquid phase and solid phase when the adsorption process reaches equilibrium. This study adopted the Langmuir, Freundlich, D–R and Temkin isotherms to describe equilibrium adsorption. Equation parameters and underlying thermodynamic assumptions

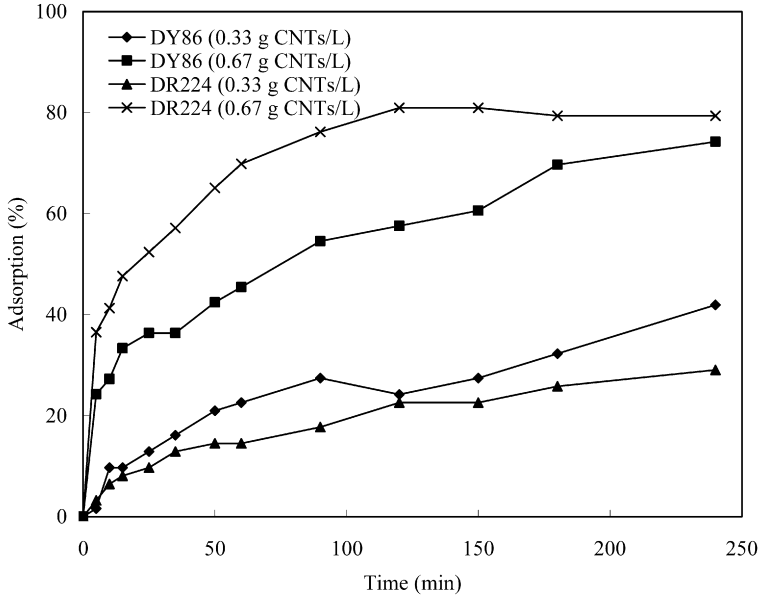

Fig. 4. Effects of CNTs dosage on the adsorption of direct dyes (dye = 10 mg/L and $T = 25\,^{\circ}\mathrm{C}$).

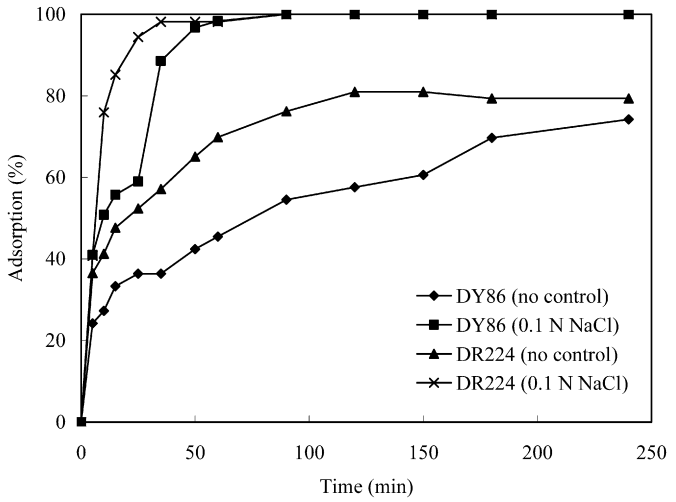

Fig. 5. Effects of ionic strength on the adsorption of direct dyes (CNTs = 0.67 g/L, dye = 10 mg/L and $T = 25\,^{\circ}\mathrm{C}$).

of these equilibrium isotherms frequently provide some insights into adsorption mechanisms, surface properties and affinities of the adsorbent. The expression for the Langmuir isotherm is

$$q_e = \frac{q_m K_L C_e}{(1 + K_L C_e)}, \tag{4}$$

where q_e is the amount of dye adsorbed per gram of CNTs (mg/g); C_e is the equilibrium concentration of dye in a solution (mg/L); K_L is the Langmuir constant (L/mg), which is related to the affinity of binding sites; and q_m is the theoretical saturation capacity of the monolayer (mg/g). The values of q_m and K_L are derived from the intercept and slope of the linear plot of $1/q_e$ versus $1/C_e$.

The Freundlich isotherm is expressed as

$$q_e = K_F C_e^{1/n}, \tag{5}$$

where q_e and C_e are defined as for the Langmuir isotherm and K_F and n are Freundlich constants, which represent adsorption capacity and adsorption strength, respectively. Both K_F and $1/n$ can be obtained from the intercept and slope of the linear plot of $\ln(q_e)$ *versus* $\ln(C_e)$. The magnitude of $1/n$ quantifies the favorability of adsorption and the degree of heterogeneity on the surface of CNTs. If $1/n$ is less than unity—suggesting favorable adsorption—adsorption capacity increases and new adsorption sites form [32].

The D–R isotherm describes adsorption on a single uniform pore. In this respect, the D–R isotherm is an analogue of the Langmuir type, but is relatively more general because it does not assume a homogeneous surface or constant adsorption potential [33,34]. The D–R isotherm can be described as follows:

$$\ln(q_e) = \ln\left(X'_m\right) - K'\varepsilon^2, \tag{6}$$

$$\varepsilon = RT \ln\left(1 + \frac{1}{C_e}\right), \tag{7}$$

$$E = (2K')^{-1/2}, \tag{8}$$

where q_e is the amount of direct dye adsorbed per unit mass of CNTs (mol/g); X'_m is adsorption capacity (mol/g); K' is a constant related to adsorption energy ($\mathrm{mol^2/kJ^2}$); R is the gas constant (kJ/mol K); T is adsorption temperature (K); ε is Polanyi potential; and E is mean free energy of adsorption (kJ/mol). The values of X'_m and K' were calculated from the intercept and slope of the $\ln(q_e)$ versus ε^2 plots. As the molecular weight of DR224 was unknown, this study assumed the molecular weight of DR224 was 600–1200 g/mol to calculate the parameters of the D–R isotherm and related thermodynamics.

The Temkin isotherm describes the behavior of adsorption systems on a heterogeneous surface, and is represented as follows:

$$q_e = \frac{RT}{b_1} \ln(K_t C_e). \tag{9}$$

Equation (9) can be expressed in a linear form as

$$q_e = B_1 \ln(K_t) + B_1 \ln(C_e), \tag{10}$$

where $B_1 = RT/b_1$, and B_1 is a constant related to adsorption heat, and K_t is the equilibrium binding constant (L/mol) corresponding to maximum binding energy. A plot of q_e versus $\ln(C_e)$ is used to determine isotherm constants.

Figs. 6 and 7 present adsorption isotherms of DY86 and DR224, respectively. Table 3 shows the isotherm parameters at different temperatures. Based on the correlation coefficient (R^2) (Table 3), the adsorption of DR86 is best fitted in the Freundlich isotherm and that of DR224 was best fitted in the D–R isotherm. Notably, K_L, K_F, B_1, $1/n$ and q_m increased as temperature increased, suggesting that the adsorption of direct dyes on CNTs increased as temperature increased (Table 3). These experimental results reveal that the affinity of binding sites for direct dyes increased as temperature increased. Since $1/n$ is less than unity, the adsorption of direct dyes onto CNTs was favored. If the E value is 8–16 kJ/mol, adsorption proceeds by ion exchange [33,34]. The E values were 9.62–12.13 kJ/mol for both DY86 and DR224 (Table 3); therefore, this work suggests that adsorption of direct dyes onto CNTs is explained by an ion-exchange process. The following section presents the detailed thermodynamic parameters.

3.4. Thermodynamic analyses

Thermodynamic parameters provide in-depth information of inherent energetic changes associated with adsorption; therefore, these parameters should be accurately evaluated. Changes to ΔG^0, ΔH^0 and ΔS^0 were calculated to elucidate the process of adsorption. The Langmuir isotherm was applied to calculate the thermodynamic parameters via Eqs. (11) and (12)

$$\Delta G^0 = -RT \ln(K_L), \tag{11}$$

$$\ln(K_L) = \frac{\Delta S^0}{R} - \frac{\Delta H^0}{RT}, \tag{12}$$

where K_L is the Langmuir equilibrium constant (L/mol); R is the gas constant (8.314×10^{-3} kJ/mol K); and T is temperature (K). Both ΔH^0 and ΔS^0 were determined from the slope and intercept of the van't Hoff plots of $\ln(K_L)$ versus $1/T$ [26,32,35]. Fig. 8 shows the regressions of van't Hoff plots. Table 4 shows the thermodynamic parameters of ΔG^0, ΔH^0 and ΔS^0. The ΔG^0 values were negative at all tested temperatures (15–55 °C), verifying that the adsorption of direct dyes onto CNTs was spontaneous and thermodynamically favorable. In other words, a more negative ΔG^0 implies a greater driving force of adsorption, resulting in increased adsorption capacity. As temperature increased from 15 to 55 °C, ΔG^0 decreased increasingly negative, suggesting that adsorption was spontaneous at high temperatures. The positive ΔH^0 values indicate that adsorption of direct dyes onto CNTs is an endothermic process, which is supported by the increase in adsorption of direct dyes as temperature increases. Furthermore, the positive ΔS^0 indicates that the degrees of freedom increased at the solid–liquid interface during adsorption of direct dyes onto CNTs. Physisorption and chemisorption can be classified, to a certain extent, by the magnitude of enthalpy change. Bonding strengths of <84 kJ/mol are typically considered as those of physisorption bonds. Chemisorption bond strengths can be 84–420 kJ/mol [36]. Generally, ΔG^0 for physisorption is less than that for chemisorption. The former is between −20 and 0 kJ/mol and the latter

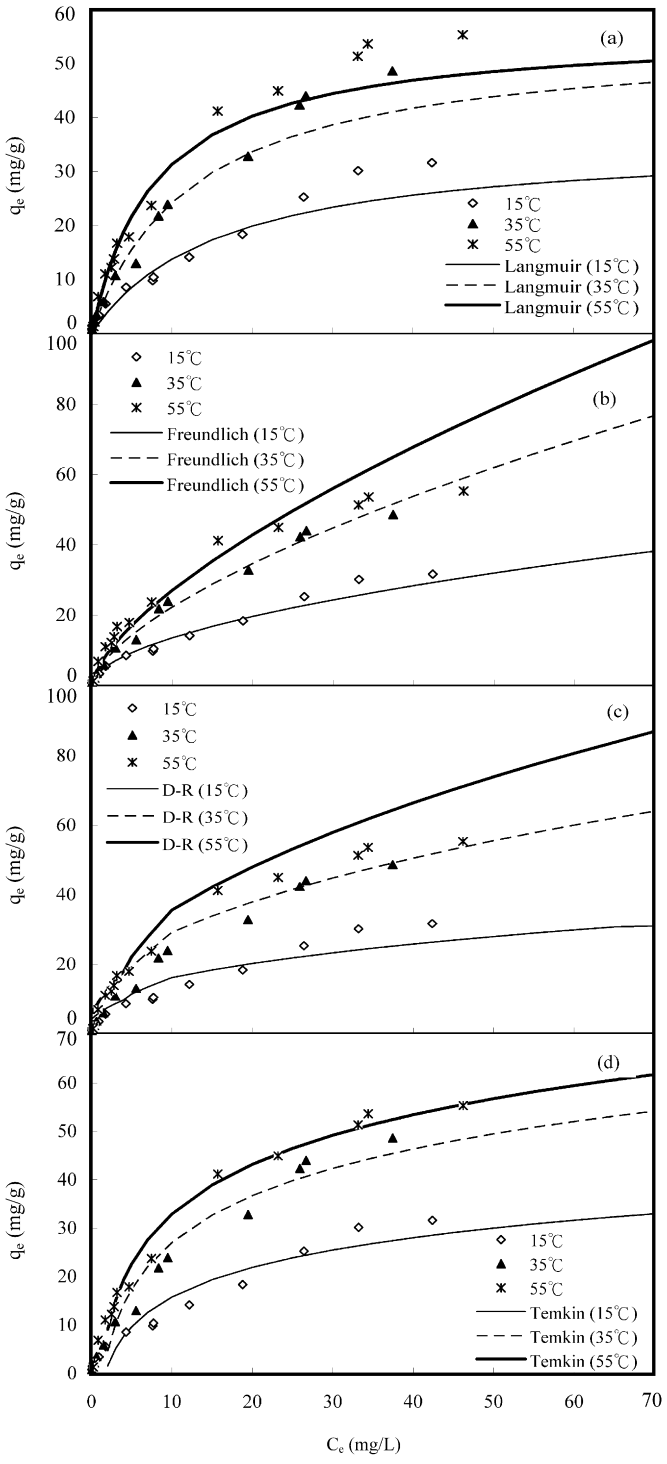

Fig. 6. Adsorption isotherm analyses of DY86: (a) Langmuir; (b) Freundlich; (c) D–R and (d) Temkin.

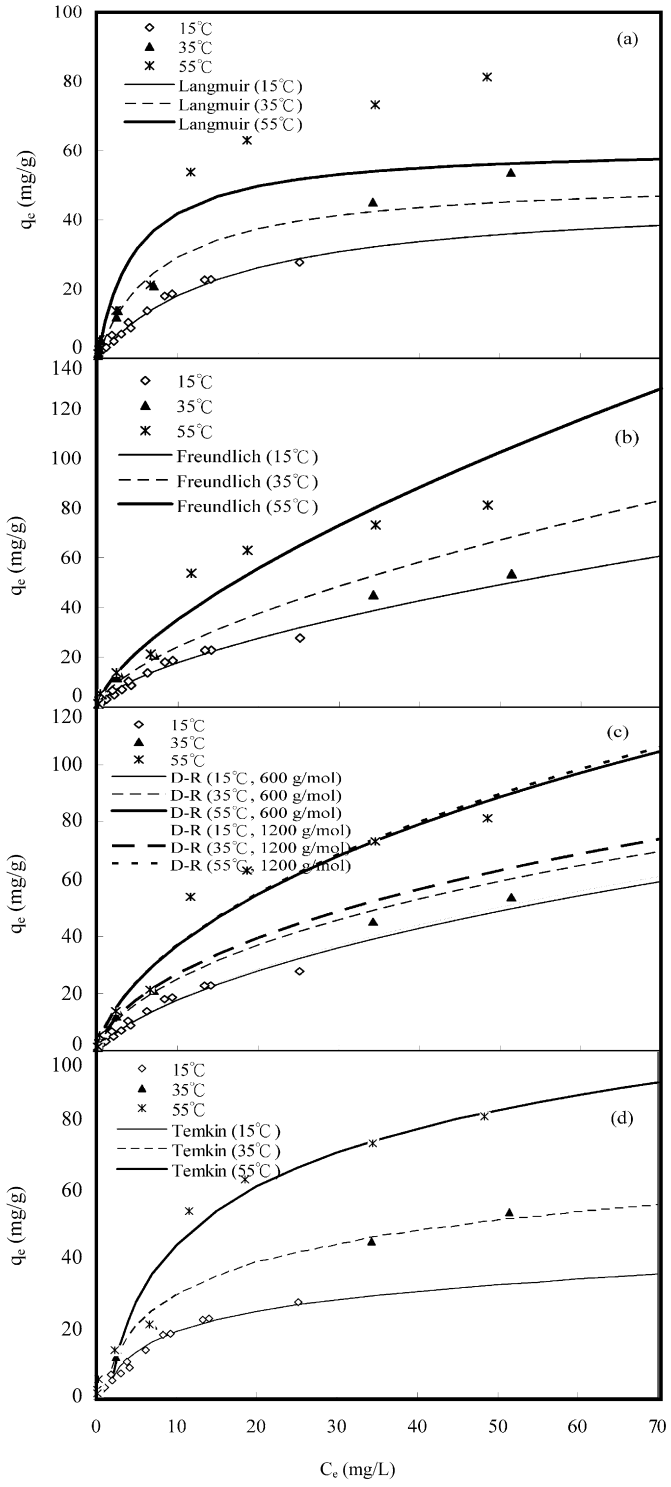

Fig. 7. Adsorption isotherm analyses of DR224: (a) Langmuir; (b) Freundlich; (c) D–R and (d) Temkin.

is between −80 and −400 kJ/mol [37]. Additionally, Nollet et al. [35] demonstrated that the physisorption process normally had activation energy of 5–40 kJ/mol, while chemisorption had a relatively higher activation energy (40–800 kJ/mol). Therefore, the values of ΔH^0, ΔG^0 and E all suggest that adsorption of direct dyes onto CNTs was driven by a physisorption process. The value of ΔH^0 for DY86 was lower than that for DR224, implying that the bond between DY86 and CNTs was weaker than that between DR224 and CNTs. Additionally, K_L, q_m, K_F and X'_m for DR224 all greater than those for DY86, implying that the affinity between DR224 and CNTs was stronger than that between DY86 and CNTs.

Table 5 compares adsorption capacity and thermodynamic parameters of direct dyes on different adsorbents in literature. Adsorption capacity of CNTs was higher than that of other adsorbents, except for soy meal hulls, bentonite and coir pith (Table 5). Differences in direct dye adsorption capacity are associated with the properties, such as structure, functional groups, pH_{pzc} and surface area, of each adsorbent. Most studies only investigated adsorption

Table 3
Isotherm parameters for the removal of direct dyes by CNTs

Langmuir constants	K_L (L/mg)	q_m (mg/g)	R^2
DY86 (15 °C)	0.062	35.8	0.904
DY86 (35 °C)	0.079	54.9	0.981
DY86 (55 °C)	0.126	56.2	0.960
DR224 (15 °C)	0.063	47.2	0.988
DR224 (35 °C)	0.128	52.1	0.971
DR224 (55 °C)	0.215	61.3	0.951
Freundlich constants	K_F	n	R^2
DY86 (15 °C)	3.96	1.87	0.990
DY86 (35 °C)	5.14	1.57	0.995
DY86 (55 °C)	5.87	1.51	0.958
DR224 (15 °C)	4.19	1.59	0.953
DR224 (35 °C)	5.61	1.58	0.955
DR224 (55 °C)	7.68	1.51	0.976
D–R constants	X'_m (mol/g)	E (kJ/mol)	R^2
DY86 (15 °C)	1.85×10^{-4}	11.95	0.977
DY86 (35 °C)	5.20×10^{-4}	11.79	0.988
DY86 (55 °C)	9.42×10^{-4}	11.79	0.978
DR224 (15 °C)[a]	$(8.2–12.5) \times 10^{-4}$	9.62–9.90	0.987
DR224 (35 °C)[a]	$(6.2–10.0) \times 10^{-4}$	11.18–11.62	0.977
DR224 (55 °C)[a]	$(9.8–15.7) \times 10^{-4}$	11.79–12.13	0.980
Temkin constants	B_1	K_t (L/mol)	R^2
DY86 (15 °C)	8.84	0.596	0.878
DY86 (35 °C)	13.96	0.694	0.943
DY86 (55 °C)	14.81	0.924	0.980
DR224 (15 °C)	8.44	0.961	0.960
DR224 (35 °C)	13.20	0.953	0.980
DR224 (55 °C)	24.04	0.628	0.938

[a] This study assumed the molecular weight of DR224 was 600–1200 g/mol to calculate the D–R isotherm parameters of DR224.

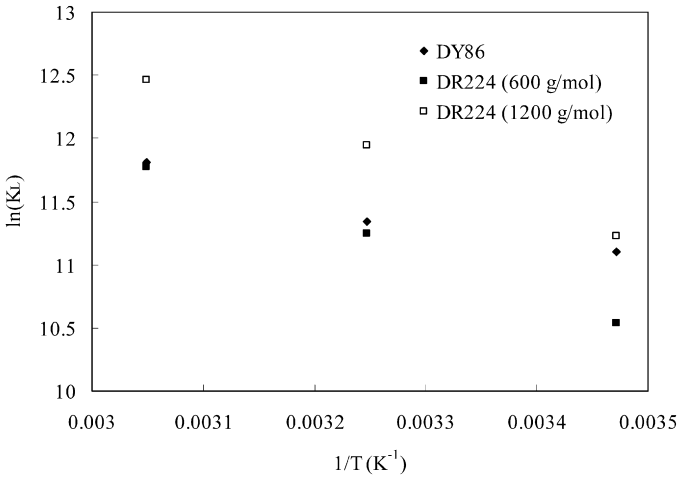

Fig. 8. Regressions of van't Hoff plots.

Table 4
Thermodynamic parameters of DY86 and DR224

	ΔG^0 (kJ/mol)	ΔH^0 (kJ/mol)	ΔS^0 (J/mol K)
DY86			
15 °C	−26.59	13.69	139.51
35 °C	−29.04		
55 °C	−32.20		
DR224			
15 °C	−25.22 ~ −26.88	24.29	172.06 ~ 177.83
35 °C	−28.81 ~ −30.58		
55 °C	−32.09 ~ −33.98		

[a] This study assumed the molecular weight of DR224 was 600–1200 g/mol to calculate the related thermodynamic parameters of DR224.

Table 5
Adsorption characteristics of direct dyes in various adsorbents

Adsorbent	Dye[a]	Adsorption capacity (mg/g)	ΔS^0 (J/mol K)	ΔH^0 (kJ/mol)	References
CNTs	DY86	56.2	139.51	13.69	This study
CNTs	DR224	61.3	172.06 ~ 177.83	24.29	This study
Coir pith	DR31	76.3	167.90	21.85	[2]
Wheat shell	DB71	46.3	242.00	42.75	[3]
Bentonite	DR2	109.9	–	–	[4]
Compost	DB71	22.0	–	–	[5]
Compost	DO39	17.0	–	–	[5]
Biogas residual slurry	DR31	3.5	32.82	11.80	[6]
Alomod shells	DR80	22.4	–	–	[7]
Orange peel	DR23	10.7	–	–	[8]
Orange peel	DR80	21.1	–	–	[8]
Soy meal hull	DR80	178.6	–	–	[9]
Soy meal hull	DR81	120.5	–	–	[9]
Fe(III)/Cr(III) hydroxide	DR31	5.0	–	–	[10]

[a] DY: Direct yellow; DR: Direct red; DB: Direct blue; DO: Direct orange.

capacity of an adsorbent and few simultaneously determined the adsorption capacity and related thermodynamics parameters. For biogas residual slurry, wheat shells and coir pith, direct dye adsorption was an endothermic process. Moreover, all adsorption of direct dyes onto different adsorbents exhibited a positive entropic change. Several investigations indicated that adsorption of dyes exhibited positive values for ΔH^0 and ΔS^0 [22,28–31].

4. Summary

This study investigated the removal of DY86 and DR224 from aqueous solution by CNTs. The amount of direct dyes adsorbed per unit CNTs mass increased with increases in initial dye concentration, CNT dosage, NaCl addition and temperature. The adsorption of DY86 and DR224 revealed that the pseudo second-order model best represented adsorption kinetics. For equilibrium adsorption, DR86 was best fitted to the Freundlich isotherm and that of DR224 was best fitted to the D–R isotherm. Based on mean free energy of adsorption, this work suggests that the adsorption of direct dyes onto CNTs can be characterized as an ion-exchange process. Moreover, the affinity between DR224 and CNTs was stronger than that between DY86 and CNTs. The results of kinetics analyses imply that adsorption of direct dyes onto CNTs involved intraparticle diffusion; however, that was not the only rate-controlling step. Thermodynamic analyses indicated that the adsorption of direct dyes onto CNTs was endothermic and spontaneous; additionally, the adsorption of direct dyes onto CNTs was via a physisorption process. This study concluded that CNTs are an appropriate adsorbent for removing direct dyes from wastewater.

Acknowledgments

The authors thank the National Science Council of the Republic of China for financially supporting this research under Contract No. NSC 94-2211-E-212-012. Additionally, the partial experiments of this research by Jyun-Ru Chen of Da-Yeh University were greatly appreciated.

References

[1] S.V. Mohan, S.V. Ramanaiah, P.N. Sarma, Biochem. Eng. J. 38 (2008) 61.
[2] M.V. Sureshkumar, C. Namasivayam, Colloids Surf. A Physicochem. Eng. Aspects 317 (2008) 277.
[3] Y. Bulut, N. Gozubenli, H. Aydin, J. Hazard. Mater. 144 (2007) 300.
[4] B. Zohra, K. Aicha, S. Fatima, B. Nourredine, D. Zoubir, Chem. Eng. J. 136 (2008) 295.

[5] L.S. Tsui, W.R. Roy, M.A. Cole, Color. Technol. 119 (2003) 14.
[6] C. Namasivayam, R.T. Yamuna, Environ. Pollut. 89 (1995) 1.
[7] F.D. Ardejani, K. Badii, N.Y. Limaee, S.Z. Shafaei, A.R. Mirhabibi, J. Hazard. Mater. 151 (2008) 730.
[8] M. Arami, N.Y. Limaee, N.M. Mahmoodi, N.S. Tabrizi, J. Colloid Interface Sci. 288 (2005) 371.
[9] M. Arami, N.Y. Limaee, N.M. Mahmoodi, N.S. Tabrizi, J. Hazard. Mater. 135 (2006) 171.
[10] C. Namasivayam, S. Sumithra, J. Environ. Manage. 74 (2005) 207.
[11] R.Q. Long, R.T. Yang, J. Am. Chem. Soc. 123 (2001) 2058.
[12] C.S. Lu, H.S. Chiu, Chem. Eng. Sci. 61 (2006) 1138.
[13] Y.H. Li, S. Wang, Z. Luan, J. Ding, C. Xu, D. Wu, Carbon 41 (2003) 1057.
[14] Y.H. Li, Z. Di, J. Ding, D. Wu, Z. Luan, Y. Zhu, Water Res. 39 (2005) 605.
[15] X. Peng, Z. Luan, Z. Di, Z. Zhang, C. Zhu, Carbon 43 (2005) 880.
[16] C.H. Wu, J. Colloid Interface Sci. 311 (2007) 338.
[17] Y.H. Li, S. Wang, X. Zhang, J. Wei, C. Xu, Z. Luan, D. Wu, Mater. Res. Bull. 38 (2003) 469.
[18] X. Peng, Z. Luan, J. Ding, Z. Di, Y. Li, B. Tian, Mater. Lett. 59 (2005) 399.
[19] C.S. Lu, Y.L. Chung, K.F. Chang, Water Res. 39 (2005) 1183.
[20] X. Peng, Y. Li, Z. Luan, Z. Di, H. Wang, B. Tian, Z. Jia, Chem. Phys. Lett. 376 (2003) 154.
[21] C.J.M. Chin, L.C. Shih, H.J. Tsai, T.K. Liu, Carbon 45 (2007) 1254.
[22] C.H. Wu, J. Hazard. Mater. 144 (2007) 93.
[23] C.S. Lu, Y.L. Chung, K.F. Chang, J. Hazard. Mater. 138 (2006) 304.
[24] I.D. Mall, V.C. Srivastava, N.K. Agarwal, Dyes Pigment 69 (2006) 210.
[25] C. Aharoni, S. Sideman, E. Hoffer, J. Chem. Technol. Biotechnol. 29 (1979) 404.
[26] A. Ozcan, E.M. Oncu, A.S. Ozcan, Colloids Surf. A Physicochem. Eng. Aspects 277 (2006) 90.
[27] A. Ozcan, A.S. Ozcan, J. Hazard. Mater. 125 (2005) 252.
[28] D. Kavitha, C. Namasivayam, Dyes Pigment 74 (2007) 237.
[29] V. Ponnusami, S. Vikram, S.N. Srivastava, J. Hazard. Mater. 152 (2008) 276.
[30] N. Thinakaran, P. Baskaralingam, M. Pulikesi, P. Panneerselvam, S. Sivanesan, J. Hazard. Mater. 151 (2008) 316.
[31] Y.S. Al-Degs, M.I. El-Barghouthi, A.H. El-Sheikh, G.M. Walker, Dyes Pigment 77 (2008) 16.
[32] A.S. Ozcan, B. Erdem, A. Ozcan, J. Colloid Interface Sci. 280 (2004) 44.
[33] A. Kilislioglu, B. Bilgin, Appl. Radiat. Isot. 58 (2003) 155.
[34] N. Unlu, M. Ersoz, J. Hazard. Mater. 136 (2006) 272.
[35] H. Nollet, M. Roels, P. Lutgen, P. Meeren, W. Verstraete, Chemosphere 53 (2003) 655.
[36] S.D. Faust, O.M. Aly, Adsorption Processes for Water Treatment, Butterworth, 1987.
[37] M.J. Jaycock, G.D. Parfitt, Chemistry of Interfaces, Ellis Horwood Ltd., Chichester, 1981.